

Approximate entropy analysis of surface electromyography for
assessing local muscle fatigue

Hong-Bo Xie^{1,3*}, Jing-Yi Guo¹, Yong-Ping Zheng^{1,2}

¹Department of Health Technology and Informatics, ²Research Institute of Innovative
Products and Technologies, The Hong Kong Polytechnic University, Hong Kong

³Department of Biomedical Engineering, Jiangsu University, Zhenjiang, China

Running Title: **Approximate entropy analysis of EMG**

***Corresponding Author:**

Hong-Bo Xie, PhD

Department of Health Technology and Informatics,

The Hong Kong Polytechnic University,

Hung Hom, Kowloon, Hong Kong SAR, P.R.China

Tel: 852-27667664

Fax: 852-23624365

Email: xiehb@sjtu.org (Dr. Hong-Bo Xie)

ypzheng@ieee.org (Dr. Yong-Ping Zheng)

Submitted to: **Annals of Biomedical Engineering**

1 **Abstract:** In the present contribution, a complexity measure is proposed to assess surface
2
3
4
5
6
7 2 electromyography (EMG) in the study of muscle fatigue during sustained, isometric muscle
8
9
10 3 contractions. Approximate entropy (ApEn) is believed to provide quantitative information about the
11
12 4 complexity of experimental data that is often corrupted with noise, short data-length, and in many cases,
13
14
15 5 has inherent dynamics that exhibit both deterministic and stochastic behaviors. We developed an
16
17 6 improved ApEn measure, i.e., fuzziness approximate entropy (*fApEn*), which utilizes the fuzzy
18
19
20 7 membership function to define the vectors' similarity. Tests were conducted on independent, identically
21
22
23 8 distributed (i.i.d.) Gaussian and uniform noises, a chirp signal, MIX processes, and Rossler, and Henon
24
25
26 9 maps. Compared with the standard ApEn, the *fApEn* showed better monotonicity, relative consistency,
27
28 10 and more robustness to noise when characterizing signals with different complexities. Performance
29
30 11 analysis on experimental EMG signals demonstrated that the *fApEn* significantly decreased during the
31
32
33 12 development of muscle fatigue, which is a similar trend to that of the mean frequency (MNF) of the
34
35
36 13 EMG signal, while the standard ApEn failed to detect this change. Moreover, the *fApEn* is more
37
38 14 sensitive to muscle fatigue than MNF with a larger linear regression slope (significant value $p=0.0213$).
39
40
41 15 The results suggest that the *fApEn* of an EMG signal may potentially become a new reliable method for
42
43
44 16 muscle fatigue assessment and be applicable to other short noisy physiological signal analysis.
45
46
47

48 18 **Keywords:** Fuzziness approximate entropy, complexity, electromyography, muscle fatigue, time series
49
50
51 19 analysis.
52
53
54 20
55
56 21
57
58
59 22
60
61
62
63
64
65

1. Introduction

Localized muscle fatigue is a complex process due to various physiological and psychological phenomena. Surface electromyography (EMG) has been widely used to detect the occurrence and development of muscle fatigue.⁸ Typically, during a sustained isometric contraction, there is an increase in the amplitude of the low frequency band and a relative decrease in the higher frequency band, which is called EMG spectrum compression. Therefore, a spectral parameter derived from the EMG signal, such as the mean frequency (MNF), is frequently used to track muscular changes.^{9, 23} Several alternative EMG spectral-based fatigue indices have been proposed to complement MNF, including changes in quartile or decile frequencies,²⁰ mode frequency¹² (frequency at the highest spectrum peak), and half-width²⁴ (spectral width at half maximum amplitude). Derivation of meaningful, statistically-significant spectral parameters requires assumptions regarding the characteristics of the signal.¹⁵ In particular, the signal must have time-invariant (stationary) or periodic frequency content within the analysis window; otherwise, the resulting spectrum will make little physical sense. Unfortunately, EMG activity can only be assumed to be locally stationary for a period of 0.5-1.5 s when the contraction level is higher than 50% of the maximal voluntary contraction (MVC).¹⁶ Moreover, in the un-fatigued state, inconsistent results have been reported: the MNF could increase, decrease or remain constant with an increasing force level.^{2, 12, 16}

EMG signals demonstrate high complexity, and mechanisms underlying the generation of EMG signals seem to be nonlinear or even chaotic in nature.^{19, 33, 36} Therefore, nonlinear time series analysis methods have been employed to derive alternate EMG-based fatigue indices. These tools may be able to provide additional information about the fatigue process. Yassierli and Nussbaum indicated that a

1 fractal-based fatigue index had sensitivity comparable to that of traditional EMG measures.³⁹ Similar
2 results were also found by Ravier et al., who used another two fractal indicators.³¹ Erfanianl et al.
3 investigated the chaotic behavior of the evoked EMG signal when the quadriceps muscles in paraplegic
4 subjects were stimulated via percutaneous intramuscular electrodes.¹⁰ They found that the correlation
5 dimension (CD) of the evoked EMG increased as the muscle became more fatigued. Stylianou et al.
6 tested the correlation integral (CI) of the EMG obtained from subjects performing isometric maximum
7 contractions until failure in elbow flexion.³⁵ The results showed that the CI is more sensitive to changes
8 in the surface EMG signal during fatigue than the spectral variables. Recurrence plot (RP) analysis is
9 another nonlinear tool for the analysis of random, chaotic, and periodic time series. The variables
10 extracted from the plots were *recurrence%*, which quantifies the signal correlations in higher
11 dimensional space, and *determinism%*, which quantifies the number of rule-obeying structures present
12 in the signal. Webber et al. demonstrated that during fatiguing contractions of the biceps brachii at
13 heavy loads, the *determinism%* of EMG increased sooner and exhibited larger changes than that of the
14 median frequency of power spectrum.³⁷

15 Though these nonlinear measures have achieved some success in quantifying EMG muscle fatigue, a
16 very large dataset is usually necessary in order to attain reliable and convergent values in calculation,
17 which may induce spurious results when applied to short or irregular sequences of real experimental
18 data.¹⁷ When dealing with surface EMG of muscle fatigue, another problem is the unavoidable noise.
19 To solve the problems of short data and noisy recordings in physiological signals, Pincus developed
20 approximate entropy (ApEn) to measure the system complexity, which is applicable to noisy and short
21 datasets.²⁵ Given N points and tolerance r , $\text{ApEn}(m, r, N)$ is approximately equal to the negative average
22 natural logarithm of the conditional probability that two sequences similar for m points within the

1 tolerance remain similar at the next point. Superior to most nonlinear measures, ApEn has shown
2 potential application to a wide range of physiological and clinical signals, such as hormone pulsatility,
3 genetic sequences, respiratory patterns, heart rate variability, electrocardiogram, and
4 electroencephalography.^{5, 7, 14, 18, 26, 27, 28} In the study of EMG signals, Ahmad and Chappell investigated
5 the approximate entropy feature of the EMG data before, during and after a muscle contraction.¹ They
6 found that there are distinct drops in the ApEn value at the start and end of a contraction, and a high
7 approximate entropy in the middle. These important findings could be extended to feature extraction
8 for an EMG control system based on pattern recognition. Radhakrishnan et al. chose ApEn as the
9 discriminating statistic for contraction segments interspersed in a uterine electromyography, which are
10 possibly nonlinear.³⁰

11 Nevertheless, ApEn values often abruptly increase up to a critical tolerance r and then decrease with
12 increased r , which makes it difficult to interpret a signal's complexity and decreases its differentiation
13 capability. In addition, ApEn suggests more similarity than is present and, thus, is biased. To be free of
14 the bias caused by self-matching, Richman and Moorman developed another related measure of time
15 series regularity named *sample entropy* (SampEn).³² However, $\text{SampEn}(m, r, N)$ is not defined if no
16 template and forward match occurs in the case of small tolerance r and data length N .³² Moreover, for
17 both ApEn and SampEn, similarity of vectors is based on a Heaviside function. The discontinuity and
18 hard boundary of a Heaviside function may cause a significant change in the SampEn value with a
19 slight change in the tolerance r , which causes problems in the validity and accuracy of the results.³²

20 In the present work, we propose an improved fuzziness approximate entropy ($f\text{ApEn}$) that measures
21 time series complexity. Compared with the standard ApEn, $f\text{ApEn}$ showed better monotonicity, relative
22 consistency, and more robustness to noise when characterizing signals with different complexities.

Moreover, for $fApEn$, there is no such restriction of the tolerance r , as in the calculation of SampEn. The $fApEn$ was then applied to characterize local muscle fatigue EMG signals. The rest of paper is organized as follows. Section II introduces the improved $fApEn$ based on the fuzzy membership function and the test signals. Section III presents the EMG experimental protocol. Section IV first makes a wide comparison of $fApEn$ and standard ApEn with regard to their ability to capture the degree of time series complexity on the test signals and then reports the results of applying $fApEn$ to characterize local muscle fatigue from EMG signals. Finally, Section V includes the discussion and conclusions.

2. Methods

2.1 Standard ApEn

For a time series T containing N data points $\{u(i): 1 \leq i \leq N\}$, the following vector sequence can be formed²⁵

$$X_i^m = \{u(i), u(i+1), \dots, u(i+m-1)\} \quad 1 \leq i \leq N-m+1 \quad (1)$$

Here, X_i^m represents m consecutive u values, commencing with the i th point. The distance d_{ij}^m between X_i^m and X_j^m is defined as

$$d_{ij}^m = d[X_i^m, X_j^m] = \max_{k \in \{0, m-1\}} |u(i+k) - u(j+k)| \quad (2)$$

For each vector X_i^m , a measure that describes the similarity between the vector X_i^m and the other vector X_j^m can be constructed as

$$C_r^m(i) = \frac{1}{N-m+1} \cdot \sum_{j=1, j \neq i}^{N-m+1} \Theta(d_{ij}^m - r) \quad (3)$$

1 where Θ is the Heaviside function

$$\Theta(z) = \begin{cases} 1, & \text{if } z \leq 0 \\ 0 & \text{if } z > 0 \end{cases} \quad (4)$$

3 The symbol r in Eq. (3) represents a predetermined tolerance value, which is defined as

$$r = k \cdot std(T) \quad (5)$$

5 where k is a constant ($k > 0$), and $std(\cdot)$ represents the standard deviation of the time series. By
6 defining

$$\phi^m(r) = \frac{1}{N-m+1} \cdot \sum_{i=1}^{N-m+1} \ln[C_r^m(i)] \quad (6)$$

8 The $ApEn$ value of the time series can be calculated as

$$ApEn(m, r) = \lim_{N \rightarrow \infty} [\phi^m(r) - \phi^{m+1}(r)] \quad (7)$$

10 For practical applications, a finite time series consisting of N data points is used to estimate the

11 $ApEn$ value of the time series, which is defined as

$$ApEn(m, r, N) = \phi^m(r) - \phi^{m+1}(r) \quad (8)$$

13 In the definition of $ApEn$,²⁵ the similarity of vectors is based on the Heaviside function shown in Eq.

14 (4). The main feature of this Heaviside function is that it provides a step function that converts the

15 input into activity equal to 0 or 1. This function is discontinuous because there is a “break” in it when

16 its value goes from 0 to 1. This leads to a type of conventional two-state classifier, which judges an

17 input pattern by whether it satisfies certain precise properties required by membership to a given class.

18 The contributions of all the data points inside the boundary are treated equally, while the data points

19 just outside the boundary are ignored. As a result, the distance d_{ij}^m that is just greater than the

20 tolerance r is not considered in $C_r^m(i)$ (or $C_r^{m+1}(i)$) and those less than the tolerance r are treated

21 equally. As a result, the $ApEn$ may not be sensitive to minor changes in signal complexity.

22

2.2 Fuzziness approximate entropy

In the physical world, however, boundaries between classes may be ambiguous, and it is difficult to determine whether an input pattern completely belongs to a class. The concept of “fuzzy sets” introduced by Zadeh proposes a means of characterizing such input–output relations in an environment of imprecision.⁴⁰ By introducing the “membership degree” with a fuzzy function $u_C(x)$, which associates each point x with a real number in the range $[0, 1]$, Zadeh’s theory provided a mechanism for measuring the degree to which a pattern belongs to a given class: the nearer the value of $u_C(x)$ to unity, the higher the membership grade of x in the set C . In *fApEn*, we employ the fuzzy membership function $u(d_{ij}^m, r)$ to obtain a fuzzy measurement of the similarity between X_i^m and X_j^m based on their shapes. As a result of the new similarity index based on the fuzzy membership function, as the hard boundary of the Heaviside function softens, the points approach each other and become more similar.

According to the new similarity index discussed above, the fuzziness approximate entropy is defined as follows. For the same time series T mentioned previously, the vector sequence takes a form similar to that of the definition of *ApEn*

$$X_i^m = \{u(i), u(i+1), \dots, u(i+m-1)\} - u0(i) \quad (i = 1, \dots, N-m+1) \quad (10)$$

However, X_i^m is generalized by removing a baseline

$$u0(i) = \frac{1}{m} \sum_{j=0}^{m-1} u(i+j) \quad (11)$$

Then, the distance d_{ij}^m between the two vectors X_i^m and X_j^m is defined as

$$d_{ij}^m = d[X_i^m, X_j^m] = \max_{k \in (0, m-1)} |u(i+k) - u0(i) - (u(j+k) - u0(j))| \quad (i, j = 1 \sim N-m+1, j \neq i) \quad (12)$$

Given r , the similarity degree D_{ij}^m between X_i^m and X_j^m is determined by a fuzzy membership function

$$D_{ij}^m = u(d_{ij}^m, r) \quad (13)$$

1 The function B_r^m is determined by

$$2 \quad C_r^m(i) = \frac{1}{N-m+1} \sum_{j=1, j \neq i}^{N-m+1} D_{ij}^m \quad (14)$$

$$3 \quad \phi^m(r) = \frac{1}{N-m+1} \cdot \sum_{i=1}^{N-m+1} \ln[C_r^m(i)] \quad (15)$$

4 Similarly, from the vector sequence $\{X_i^{m+1}\}$ and the function $\phi^{m+1}(r)$, we can define the measure
5 $fApEn(m, r)$ of the time series as

$$6 \quad fApEn(m, r) = \lim_{N \rightarrow \infty} [\phi^m(r) - \phi^{m+1}(r)] \quad (16)$$

7 Finally, for finite datasets, $fApEn$ can be estimated from the statistic

$$8 \quad fApEn(m, r, N) = \phi^m(r) - \phi^{m+1}(r) \quad (17)$$

9 In practice, a Gaussian function, Sigmoid function, bell shape function, or any other fuzzy
10 membership function that possesses the following desired properties can be chosen to describe the two
11 vectors' similarities: 1) continuity, so that the similarity does not change abruptly; and 2) convex, so
12 that self-similarity is the maximum. In the present study, the following Gaussian function was
13 employed as the fuzzy membership function for the $fApEn$ calculation.

$$14 \quad u(d_{ij}^m, r) = \exp(-d_{ij}^2 / r) \quad (18)$$

15 As suggested by Pincus,²⁵ the vector dimension m is set to 2 to calculate both the $fApEn$ and $ApEn$.

17 2.3 Simulated signals

19 The ability of the proposed method to capture different degrees of complexity was tested on several
20 types of simulations to reproduce both stochastic and deterministic short time series. The simulated
21 signals include independent, identically distributed (i.i.d.) Gaussian and uniform noise, a chirp signal,
22 MIX processes, and Rossler, and Henon maps. Informally, the MIX(P) time series of N points, where P

is between 0 and 1, is a sine wave, where $N \times P$ randomly chosen points have been replaced with random noise.³² The Rossler map is given by³⁴

$$\frac{dx}{dt} = -z - y \quad (19)$$

$$\frac{dy}{dt} = x + 0.15y \quad (20)$$

$$\frac{dz}{dt} = 0.20 + R(zx - 5.0) \quad (21)$$

Time series were obtained for $R = 0.7, 0.8$, and 0.9 by integration via an explicit time-step method with an increment of 0.005 . The y values were recorded at intervals of $\Delta t = 2$. The respective system dynamics with three different R values are given by a twice-periodic, four-times-periodic, and chaotic limit cycle with increasing complexity.²⁵

A parameterized version of the Henon map is given by²⁹

$$x_{i+1} = Ry_i + 1 - 1.4x_i^2 \quad (22)$$

$$y_{i+1} = 0.3Rx_i \quad (23)$$

Time series for x_i were obtained for $R=0.8, 0.9$ and 1.0 with increasing complexity.²⁵

14

3. Experimental protocol

16

The EMG signals analyzed in this paper were recorded during the voluntary isometric contractions of twelve healthy human subjects (eight males and four females, age: 30.2 ± 4.9). None of them had history of any neuromuscular disorder and each gave written informed consent prior to the experiment. A pair of surface EMG self adhesive conductive gel electrodes (Axon Systems, Inc., New York, USA), with their centers 25 mm apart from each other, were placed longitudinally on abraded, clean skin, immediately under the thickest point of the biceps. The EMG reference electrode was placed on the

proximal head of the ulna. When the experiment began, the subject was asked to perform an elbow flexion against the lever arm to 80% of his/her maximal voluntary contraction (MVC) and maintain this value through visual feedback of the torque reading on the screen. The test was stopped when the torque dropped to approximately 70% of the MVC, which indicates the muscle is fatigued. The gain of the EMG signal was 2000 with a 10–400 Hz bandwidth. Signals from the EMG electrodes were sampled at 1 KHz and stored in the computer for further analysis.

4. Results

4.1 Continuity and greater parameter selection freedom

In the first simulation, the input series were separately obtained as a realization of Gaussian and uniform noise. Figs. 1 and 2 depict the performances of ApEn, SampEn, f ApEn on i.i.d Gaussian and uniform noise, respectively. Two short data lengths, i.e., $N=50$ and 100, were considered for each noise type. For both noise types, SampEn gave no entropy values when the tolerance r was smaller than about 0.1 for $N=100$, as shown in the right panels of Figs. 1 and 2, and 0.15 for $N=50$ in the left panels. Therefore, the calculation of SampEn is confronted with the parameter limitation, and as the length of the dataset decreases, the minimum tolerance r needed increases. However, this problem does not affect the calculation of ApEn and f ApEn. Due to the lack of entropy values for comparison, we just consider ApEn and f ApEn for the remainder. In addition, within a certain tolerance range, the values of ApEn and SampEn increased or decreased abruptly with a slight change in r , so both of them exhibit discontinuity. This problem does not bother f ApEn, whose values change smoothly and continuously

with increasing r .

4.2 Relative consistency and monotonicity

An essential feature of the complexity measures is their relative consistency. That is, if a series is more complex than another, then it should have higher entropy statistics for all tested conditions.

Graphically, plots of $fApEn$ as a function of r for different series should not cross over one another. We first tested this expectation using the realizations of the $MIX(P)$ process, where the degree of complexity could be specified. The strategy was to compare $MIX(0.3)$, $MIX(0.5)$, and $MIX(0.7)$ series. The expected result was that $fApEn(MIX(0.3))$ should be less than $fApEn(MIX(0.5))$, while $fApEn(MIX(0.5))$ should be less than $fApEn(MIX(0.7))$. Fig. 3 shows the test results with 100-point realizations of the $MIX(P)$ process for $fApEn$ and standard $ApEn$. Obviously, for each tolerance value r , the $fApEn$ of $MIX(0.3)$ was significantly and strictly lower than that of $MIX(0.5)$, while $MIX(0.5)$ was lower than $MIX(0.7)$, which demonstrated the relative consistency of $fApEn$ in the test. However, for $ApEn$, the plots of the three series cross over several times and the entropy values were almost equal in some range of r , which indicates the loss of relative consistency of $ApEn$ in the test.

The lack of relative consistency of $ApEn$ was studied by Chen et al. using Gaussian noise and a chirp signal.⁵ We also tested the performance of $fApEn$ using Gaussian noise and a chirp signal. Fig. 4 shows the results of $fApEn$ and $ApEn$ with 500-point realizations of the Gaussian noise and chirp signal. The misleading results of $ApEn$ shown in Fig. 4(b) were similar to those of Chen et al., i.e., the complexity value of $ApEn$ for the chirp signal is larger than the white noise signal when r is lower than 0.15. However, the $fApEn$ could distinguish the complexity of the pair series correctly with relative

1 consistency. We also test the pair series with shorter data lengths. For ApEn, it was found that as the
2 length decreases, the value of r at the cross point of the pair plots increases. This means that the ApEn
3 could not distinguish the complexity of the pair series for smaller r . However, the f ApEn still possessed
4 relative consistency, even when $N=100$ for the Gaussian noise and chirp signal.

5 Observing the plots from Fig. 1 to Fig. 4, no matter which signal was considered, the f ApEn values
6 monotonically decreased as r increased (with a slight violation for the two noise series with rather short
7 length $N=50$ and small tolerance r). However, ApEn values often abruptly increased up to a critical r
8 and then decreased as r increased. The lack of monotonicity of ApEn leads to the difficulty of
9 interpreting a signal's complexity and reduced its differentiation capability.

10

11 *4.3 Robustness to noise*

12

13 In this section, we assess the performance of f ApEn against noise contamination, which is a key
14 feature of practical application to noisy data sets. This property of both f ApEn and standard ApEn was
15 tested using two low-dimensional nonlinear deterministic systems: the Rossler map and the Henon map
16 superimposed with different levels of white noise. Series of systems, each with a control parameter R ,
17 were generated after a transient period of 1000 points. Noise was superimposed on each time series
18 through the addition of i.i.d. Gaussian white noise with different noise levels (NL).

19 For each system, the statistics of both f ApEn and standard ApEn were calculated for time series
20 with different lengths as r varied from 0.01 to 1. The more complex Rossler and Henon systems
21 produce larger entropy values, which are true to both f ApEn and standard ApEn if N and r are large
22 enough. However, when the values of N and r were small, the complexity measured by the

1 conventional ApEn tilted and the results were even worse when noise was superimposed. Fig. 5 and Fig.
2 6 show entropy values of the Rossler and Henon maps contaminated with noise ($NL = 0.1$). The series
3 length of the Rossler map was $N = 500$ for the calculation of entropy values in this test and $N = 100$ for
4 the Henon map. It was found that $fApEn$ distinguished both Rossler and Henon map systems in the
5 whole span as r ranged from 0.01 to 1 in steps of 0.01. However, the ApEn could only distinguish the
6 Henon map contaminated by noise with a noise level of 0.1 for r ranging from about 0.1 to 0.6, and
7 failed for Rossler map, independent of the value of r . Fig. 7 and 8 show the performances of the two
8 entropy statistics that distinguish Rossler and Henon systems at different noise levels ($r = 0.1$). $fApEn$
9 could correctly distinguish the series generated by both Rossler and Henon maps with different control
10 parameters R until the noise level increased to 0.5. However, it was difficult for ApEn to distinguish
11 Rossler system contaminated by noise for $r = 0.1$ and $N = 500$. For the Henon system, ApEn could
12 differentiate the system complexity only when the superimposed noise level was less than 0.2. Thus,
13 $fApEn$ showed better robustness to noise contamination in distinguishing the nonlinear system
14 dynamics.

16 *4.4 Performance on EMG signal*

18 To demonstrate the potential applicability of our proposed method, the $fApEn$ and ApEn of EMG
19 signals were tested as indicators of local muscle fatigue during sustained isometric contraction. The
20 EMG signal is the electrical manifestation of the neuromuscular activation associated with muscle
21 contraction.³⁸ Fig. 9 shows a typical raw EMG signal acquired from subject 2. The reduced variation
22 between slow and fast twitching motor units and the firing synchronization suggest that the complexity

1 of the EMG signal decreases as fatigue sets in. Therefore, it is expected that the values of both $fApEn$
2 and $ApEn$ decrease as muscle fatigue develops.

3 In order to monitor the changes of $fApEn$ and $ApEn$ of EMG over time, the EMG signal was first
4 segmented into consecutive, non-overlapped epochs that were 500 ms in length. For each epoch, the
5 EMG signal was normalized and the procedure described above was conducted to calculate both $fApEn$
6 and $ApEn$. Fig. 10 (a) and (b) show the time course of the two measures for subject 2. It is observed
7 that the $fApEn$ decreased significantly during the development of muscle fatigue. Unfortunately, there
8 are only three different $ApEn$ values for different EMG epochs. The $ApEn$ failed to detect the subtle
9 pattern changes of EMG signals recorded during muscle fatigue. The results from all the other subjects
10 with different epoch lengths were similar to the results shown in Fig. 10 (a) and (b), indicating that the
11 $fApEn$ of EMG could qualify as a new indicator of muscle fatigue.

12 Mean frequency so far has been hailed as the gold standard for muscle fatigue assessment by using
13 EMG under 'static' conditions.²² The slope of the linear regression for the time course of MNF has
14 served as an important quantitative fatigue index.^{11,38} In order to further examine the effectiveness of
15 the $fApEn$ statistic for muscle fatigue assessment, the MNF analysis was also applied to the EMG
16 signals for comparison. The time course of the MNF of subject 2 with 500 ms epoch is shown in Fig.
17 10(c). A similar time-decrease trend between $fApEn$ and MNF was observed. To facilitate the
18 comparison of the effectiveness, the $fApEn$ and MNF were normalized by their respective first epoch
19 values. A least-square error linear regression was then fitted to each normalized $fApEn$ and MNF over
20 the period of the contraction to obtain the slope. Table 1 gives the slopes of the $fApEn$ and MNF for
21 each subject. One-way ANOVA was performed to assess the statistical significance of the results. It was
22 found that the slope of $fApEn$ was significantly higher than that of the MNF ($p = 0.0213$). The results

1 suggested that $fApEn$ should be superior to MNF in monitoring muscle fatigue because the higher slope
2 indicates that the index is more sensitive to the fatigue phenomenon.

3 4 **5. Discussion and conclusions**

5
6 In the present work, we aimed to characterize the complexity changes of local muscle fatigue.
7 Approximate entropy is a widely used method to provide a general understanding of the complexity of
8 a time series and is theoretically related to Kolmogoro-Sinai entropy. Its popularity stems from the fact
9 that it can be applied to both short and noisy data recordings, and it is relatively easy to use.
10 Consequently, it has been widely utilized in processing various biological data including EMG signals.
11 Sample entropy was developed to overcome the self-match problem associated with ApEn. However,
12 SampEn often fails in the practical applications because the value is undefined when the tolerance r is
13 small. In addition, the lack of relative consistency and monotonicity in ApEn causes difficulty in
14 interpreting the signal's complexity and reduces its differentiation capability. Lu et al. recently
15 advocated finding the maximum ApEn by assessing all values of r from 0 to 1 to interpret the signal's
16 complexity²¹ and proposed a method to select the maximum ApEn value for a given signal. However,
17 the procedure of finding the maximum ApEn is cumbersome and time consuming with additional
18 computational burden. In this contribution, by employing fuzzy membership function, fuzziness
19 approximate entropy was proposed as an improved method to quantify the time series complexity.
20 $fApEn$ changes the rule that determines vector similarity in ApEn and SampEn, which are both based
21 on a Heaviside function. Unlike the hard and discontinuous boundary of a Heaviside function, the soft
22 and continuous boundary of a fuzzy membership function makes the $fApEn$ statistics decrease

smoothly and monotonically when there is a slight increase in the tolerance r . Moreover, the $fApEn$ statistic also shows better relative consistency and robustness to noise, and a shorter data length is needed to distinguish different processes. Therefore, the fuzziness approximate entropy statistic provides an improved evaluation of time series complexity, and can thus be more conveniently and powerfully applied to noisy physiological signals with short data length.

Frequency analysis of EMG signals in particular has been recognized as a useful tool to measure local muscle fatigue. Due to the reduction in the muscle fiber conduction velocity and increased motor unit synchronization and recruitment, there is a significantly lower shift of the fatigue EMG power spectrum.⁸ Pincus has already found that there is often a relationship between entropy and the power spectrum measure, where larger entropy corresponds to broader banded spectra, and smaller entropy corresponds to more peaked spectra.²⁷ In the present work, when the $fApEn$ was applied to EMG analysis during the static isometric fatigue, the results were consistent with the Pincus' conclusion. That is, both $fApEn$ and MNF decrease significantly with the development of local muscle fatigue. However, the standard $ApEn$ could not detect the complexity change in the EMG signal with three values close to zero. This may due to the following two factors. First, EMG is a complex physiological signal with broad band width (10-500 Hz), which results in fewer template matches of vectors X_i^m and X_j^m . The most template matches of the different EMG epoch signal come from the self-match, which leads to the smallest difference between $C_r^m(i)$ and $C_r^{m+1}(i)$. Then, according to its definition, the distance d_{ij}^m is less than the tolerance r of the obtained template match and is equally treated in $C_r^m(i)$ (or $C_r^{m+1}(i)$) independent of the difference between the vectors X_i^m and X_j^m . Compared with the conventional MNF variable, the slope of the $fApEn$ linear regression is significantly sharper for the EMG signal. The EMG frequency spectrum character analysis is based on the assumption that

the EMG signal is a linear stationary stochastic process. It has been recently recognized that EMG signals exhibit high-dimensional nonlinear characteristics.^{19, 33, 36} *fApEn* is applicable to both noisy and non-stationary time series, irrespective of whether their origin is linear stochastic or nonlinear deterministic.¹³ The nonlinear characteristics of EMG fatigue could be revealed by using *fApEn* analysis, but they are not captured by the linear transform spectrum variable MNF. Our results are in accordance with the recurrence quantification analysis of EMG by Webber et al., and correlation integral analysis by Stylianou et al.^{35, 37} The nonlinear measures often show higher sensitivity than the linear method, such as the spectrum variable that monitors muscle fatigue.

In the present work, the proposed *fApEn* was only applied to an EMG signal during static isometric contractions. Although the fatigue analysis of the EMG signal detected during constant-force isometric contractions has been useful in a number of applications, it is evident that the isometric contractions are not typical in most daily activities. Wavelet and Cohen class time-frequency representations have been adopted as the primary techniques to analyze dynamic tasks.^{3, 4} To reduce the variability of the instantaneous spectral estimates by the above techniques, the EMG of a dynamic contraction is always assumed to be quasi-stationary or quasi-cyclostationarity.⁴ However, as mentioned before, such an assumption is not needed for the fuzziness approximate entropy measure. In the next step, the *fApEn* analysis of the EMG signal during dynamic contraction and its comparison with instantaneous spectral variables should be considered to extend its applicability in sports medicine, ergonomics, and rehabilitation.

Acknowledgements

This work was partially supported by the Hong Kong Research Grant Council (PolyU 5331/06E), The

1 Hong Kong Polytechnic University (1-BB69), The natural science foundation of Jiangsu Province
2
3
4
5
6
7 (2009A195), and Jiangsu University, PRC (07JDG40).
8
9

10
11
12
13
14
15
16
17
18
19
20
21
22
23
24
25
26
27
28
29
30
31
32
33
34
35
36
37
38
39
40
41
42
43
44
45
46
47
48
49
50
51
52
53
54
55
56
57
58
59
60
61
62
63
64
65

4 **References**

- 5
6 1. Ahmad, S. A., and P. H. Chappell. Moving approximate entropy applied to surface
7 electromyographic signals. *Biomed. Sig. Process. & Contr.* 3: 88–93, 2008.
8
9 2. Bilodeau, M., S. Schindler-Ivens, D.M. Williams, R. Chandran, and S.S. Sharma. EMG frequency
10 content changes with increasing force and during fatigue in the quadriceps femoris muscle of men
11 and women. *J. Electromyogr. Kinesiol.* 13: 83–92, 2003.
12
13 3. Bonato, P. Recent advancements in the analysis of dynamic EMG data. *IEEE Med. Biol. Mag.*
14 20(6): 29–32, 2001.
15
16 4. Bonato, P., S. H. Roy, M. Knaflitz, and C. J. De Luca. Time-frequency parameters of the surface
17 myoelectric signal for assessing muscle fatigue during cyclic dynamic contractions. *IEEE Trans.*
18 *Biomed. Eng.* 48: 745–753, 2001.
19
20 5. Caldirola, D., L. Bellodi, A. Caumo, G. Migliarese, and G. Perna. Approximate entropy of
21 respiratory patterns in panic disorder. *Amer. J. Psychiatry.* 161: 79–87, 2004.
22
23 6. Chen, X.N., I. Solomon, and K.H. Chon. Comparison of the use of approximate entropy and
24 sample entropy: applications to neural respiratory signal. *Proceedings of the 2005 IEEE EMBS 27th*
25 *Annual Conference.* Shanghai, 2005, pp. 4212–4215.
26
27 7. Christen, J. A., J. L. Torres, and J. Barrera. A statistical feature of genetic sequences. *Biometrical*
28 *J.* 40: 855–863, 1998.

- 1 8. DeLuca, C. J. Myoelectric manifestations of localized muscular fatigue in humans. *Crit. Rev.*
2
3
4
5
6
7
8
9
10 9. Duchene, J., and F. Goubel. Surface electromyogram during voluntary contraction: processing
11
12 4 tools and relation to physiological events. *CRC Crit. Rev. Biomed. Eng.* 21: 313–397, 1993.
13
14
15 10. Erfanian, A., H.J. Chizeck, and R.M. Hashemi. Chaotic activity during electrical stimulation of
16
17 6 paralyzed muscle. *18th Annal International Conference of the IEEE EMBS*, Amsterdam, 1996. pp.
18
19 7 1756–1757.
20
21
22
23 11. Georgakis, A., L.K. Stergioulas, and G. Giakas. Fatigue analysis of the surface EMG signal in
24
25 9 isometric constant force contractions using the averaged instantaneous frequency. *IEEE Trans on*
26
27 10 *Biomed. Eng.* 50(2): 262–265, 2003.
28
29
30 12. Hagg, G.M. Interpretation of EMG spectral alterations and alteration indexes at sustained
31
32 12 contraction. *J Appl Physiol*, 73(3): 1211–1217, 1992.
33
34
35 13. Hornero, R., D. Abasolo, J. Escudero, and C. Gomez. Nonlinear analysis of electroencephalogram
36
37 14 and magnetoencephalogram recordings in patients with Alzheimer's disease. *Phil. Trans. R. Soc. A.*
38
39 367(1887): 317–336, 2009.
40
41
42
43 14. Hu, X., C. Miller, P. Vespa, and M. Bergsneider. Adaptive computation of approximate entropy
44
45 17 and its application in integrative analysis of irregularity of heart rate variability and intracranial
46
47 18 pressure signals. *Med. Eng & Phys.* 30: 631–639, 2008.
48
49
50
51 15. Huang, N.E., Z. Shen, S.R. Long, M.L.C. Wu, H.H. Shih, Q.N. Zheng, N.C. Yen, C.C. Tung, and
52
53 20 H.H. Liu. The empirical mode decomposition and the Hilbert spectrum for non-linear and
54
55 21 non-stationary time series analysis. *Proc. Roy. Soc. Lond. Ser. A: Math. Phys. Eng. Sci.* 454:
56
57 903–995, 1998.
58
59
60
61
62
63
64
65

- 1 16. Karlsson, S., N. O stlund, B. Larsson, and B. Gerdle. An estimation of the influence of force
2 decrease on the mean power spectral frequency shift of the EMG during repetitive maximum
3 dynamic knee extensions. *J. Electromyogr. Kinesiol.* 13: 461–468, 2003.
- 4 17. Katsev, S., and I. L’Heureux. Are Hurst exponents estimated from short or irregular time series
5 meaningful? *Comput. & Geosci.* 29: 1085–1089, 2003.
- 6 18. Koskinen, M., T. Seppanen, S. Tong, S. Mustola, and N. V. Thakor. Monotonicity of approximate
7 entropy during transition from awareness to unresponsiveness due to propofol anesthetic
8 induction. *IEEE Trans. Biomed. Eng.* 53(4): 669–675, 2006.
- 9 19. Lei, M., Z.Z. Wang, and Z.J. Feng. Detection nonlinearity of action surface EMG signal. *Phys.*
10 *Lett. A.* 290: 297–303, 2001.
- 11 20. Linssen, W.H., D.F. Stegeman, E.M. Joosten EM, M.A. van’t Hof, R.A. Binkhorst, and S.L.
12 Notermans. Variability and interrelationships of surface EMG parameters during local muscle
13 fatigue. *Muscle Nerve.* 16: 849–56, 1993.
- 14 21. Lu, S., X.N. Chen, J.K. Kanters, I.C. Solomon, and K.H. Chon. Automatic selection of the
15 threshold value r for approximate entropy. *IEEE Trans. Biomed. Eng.* 55(8): 1966–1972, 2008.
- 16 22. MacIsaac, D.T., P.A. Parker, K.B. Englehart, and D.R. Rogers. Fatigue estimation with a
17 multivariable myoelectric mapping function. *IEEE Trans Biomed Eng.* 53(4): 694–700, 2006.
- 18 23. Merletti, R., M. Knaflitz, and C. Deluca. Myoelectric manifestations of fatigue in voluntary and
19 electrically elicited contractions. *J. Appl. Physiol.* 69: 1810–1820, 1990.
- 20 24. Nargol, A.V., A.P. Jones, P.J. Kelly, and C.G. Greenough CG. Factors in the reproducibility of
21 electromyographic power spectrum analysis of lumbar paraspinal muscle fatigue. *Spine.* 24(9):
22 883–888, 1999.

- 1 25. Pincus, S.M. Approximate entropy as a measure of system complexity. *Proc. Nat. Acad. Sci. USA*.
2
3
4
5
6
7 88: 2297–2301, 1991.
8
9
10 26. Pincus, S.M. Approximate entropy in cardiology. *Herzschr Elektrophys*. 11:139–150, 2000.
11
12 27. Pincus, S.M. Approximate entropy as a measure of irregularity for psychiatric serial metrics.
13
14
15 *Bipolar Disorders*. 8: 430–440, 2006.
16
17 28. Pincus, S.M., and D. L. Keefe. Quantification of hormone pulsatility via an approximate entropy
18
19
20 algorithm. *Amer. J. Physiol.—Endocrinol. Metabolism*. 262: E741–E754, 1992.
21
22
23 29. Radhakrishnan, N., and B.N. Gangadhar. Estimating regularity in epileptic seizure time-series.
24
25
26 *IEEE Eng. Med. Biol. Mag.* 17(3): 89–94, 1998.
27
28 30. Radhakrishnan, N., J. D. Wilson, C. Lowery, P. Murphy, and H. Eswaran. Testing for nonlinearity
29
30
31 of the contraction segments in uterine electromyography. *Int. J. Bifurcationd Chaos Appl. Sci.*
32
33 *Eng.* 10: 2785–2790, 2000.
34
35 31. Ravier, P., O. Buttelli, R. Jennane, and P. Couratier. An EMG fractal indicator having different
36
37
38 sensitivities to changes in force and muscle fatigue during voluntary static muscle contractions. *J.*
39
40
41 *Electromyogr. Kinesiol.* 15: 210–221, 2005.
42
43 32. Richman, J. S., and J. R. Moorman. Physiological time-series analysis using approximate and
44
45
46 sample entropy. *Amer. J. Physiology—Heart Circulatory Physiology*. 278: H2039–H2049, 2000.
47
48 33. Rodrick, D., and W. Karwowski. Nonlinear dynamical behavior of surface electromyographical
49
50
51 signals of biceps muscle under two simulated static work postures. *Nonlinear Dynamics,*
52
53
54 *Psychology, Life Sci.* 10: 21–35, 2006.
55
56 34. Rossler, O.E. An equation for continous chaos. *Phys. Lett. A*. 57: 397-398, 1976.
57
58
59 35. Stylianou, A. P., C. W. Luchies, D. E. Lerner, and G. W. King. The use of correlation integrals in
60
61
62
63
64
65

- the study of localized muscle fatigue of elbow flexors during maximal efforts. *J. Electromyogr. Kinesiol.* 15: 437–443, 2005.
36. Swie, Y. W., K. Sakamoto, and Y. Shimizu. Chaotic analysis of electromyography signal at low back and lower limb muscles during forward bending posture. *Electromyogr. Clinical Neurophysiol.* 45: 329–342, 2005.
37. Webber, Jr. C.L., M.A. Schmidt, and J.M. Walsh. Influence of isometric loading on biceps EMG dynamics as assessed by linear and non-linear Tools. *J. Appl. Physiol.* 78 (3): 814–822, 1995.
38. Xie, H.B., and Z.Z. Wang. Mean frequency derived via Hilbert-Huang transform with application to fatigue EMG signal analysis. *Comput. Meth. Programs Biomed.* 82(2): 114–120, 2006.
39. Yassierli, and M. A. Nussbaum. Utility of traditional and alternative EMG-based measures of fatigue during low-moderate level isometric efforts. *J. Electromyogr. Kinesiol.* 18: 44–53, 2008.
40. Zadeh, L.A. Fuzzy sets. *Information Control.* 8: 338–353, 1965.

1 **Figure captions**

2 Figure. 1 $fApEn(2,r,N)$, $ApEn(2,r,N)$, and $SampEn(2,r,N)$ as functions of r for i.i.d.
3 Gaussian-distributed noise as r varies from 0.01 to 1.0 in steps of 0.01. The data length is $N=50$ (a), and
4 $N=100$ (b).

5 Figure. 2 $fApEn(2,r,N)$, $ApEn(2,r,N)$, and $SampEn(2,r,N)$ as functions of r for i.i.d. uniformly
6 distributed noise as r varies from 0.01 to 1.0 in steps of 0.01. The data length is $N=50$ (a), and $N=100$
7 (b).

8 Figure. 3 The performances of $fApEn(2, r, N)$ (a), and $ApEn(2, r, N)$ (b) statistics that measure the
9 complexity of MIX(0.3), MIX(0.5) and MIX(0.7) for $N=100$.

10 Figure. 4 The performances of $fApEn(2, r, N)$ (a), and $ApEn(2, r, N)$ (b) statistics that measure the
11 complexity of an i.i.d. Gaussian distributed noise and chirp signal for $N=500$.

12 Figure. 5 The performances of $fApEn(2, r, N)$ (a), and $ApEn(2, r, N)$ (b) statistics that distinguish
13 Rossler systems at a noise level of 0.1. The parameters used for the calculation are $N= 500$ and $m = 2$.

14 Figure. 6 The performances of $fApEn(2, r, N)$ (a), and $ApEn(2, r, N)$ (b) statistics that distinguish
15 Hennon systems at a noise level of 0.1. The parameters used for the calculation are $N= 100$ and $m = 2$.

16 Figure. 7 The performances of $fApEn(2, r, N)$ (a), and $ApEn(2, r, N)$ (b) statistics that distinguish
17 Rossler systems at $r=0.1$. The parameters used for the calculation are $N= 500$ and $m = 2$.

18 Figure. 8 The performances of $fApEn(2, r, N)$ (a), and $ApEn(2, r, N)$ (b) statistics that distinguish
19 Hennon systems at $r=0.1$. The parameters used for the calculation are $N= 100$ and $m = 2$.

20 Figure. 9 The time course of EMG signals recorded from the biceps during the static isometric
21 contraction from non-fatigue to exhaustion for subject 2.

22 Figure. 10 Time courses of the $fApEn$ (a), $ApEn$ (b), and MNF (c) for the EMG of subject 2 shown in

1 Fig. 9. The analysis window was 500 ms. The linear regressions of *f*ApEn (a) and MNF (c) are
2
3
4
5
6
7
8
9
10
11
12
13
14
15
16
17
18
19
20
21
22
23
24
25
26
27
28
29
30
31
32
33
34
35
36
37
38
39
40
41
42
43
44
45
46
47
48
49
50
51
52
53
54
55
56
57
58
59
60
61
62
63
64
65

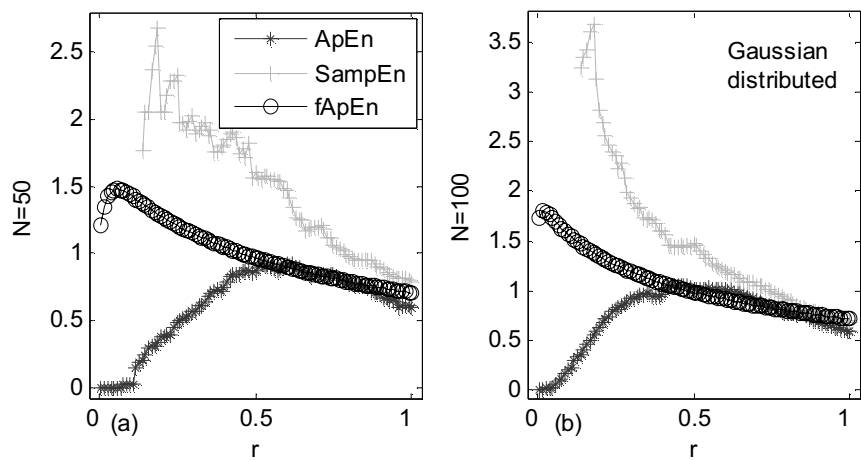


FIGURE 1.

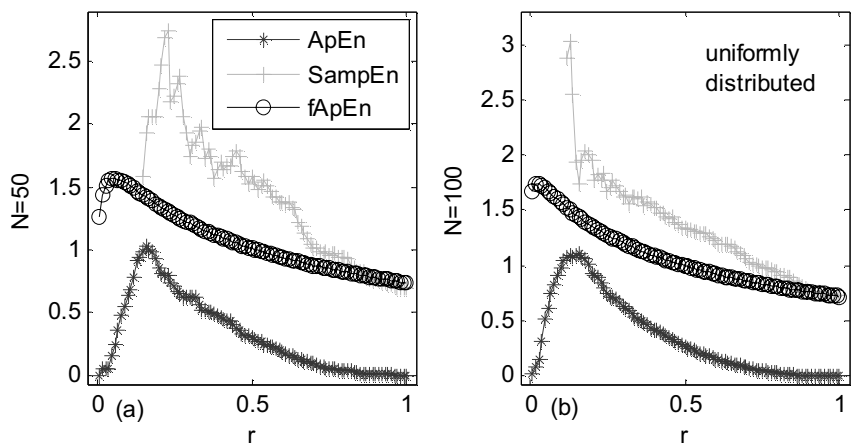


FIGURE 2.

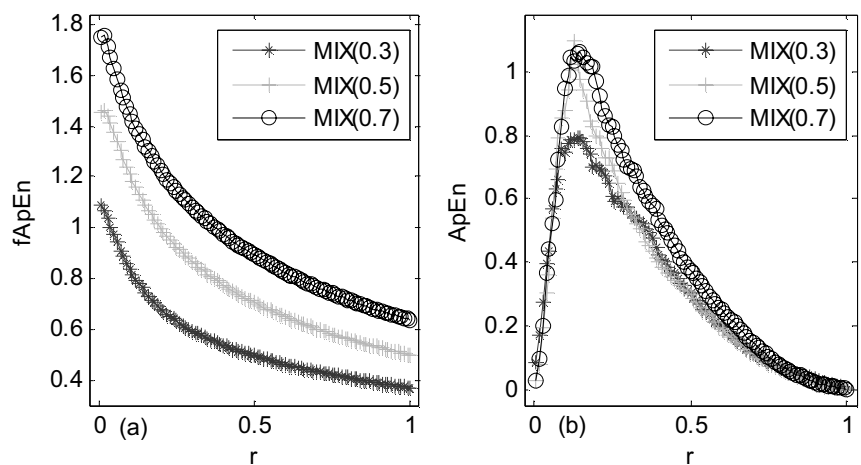


FIGURE 3.

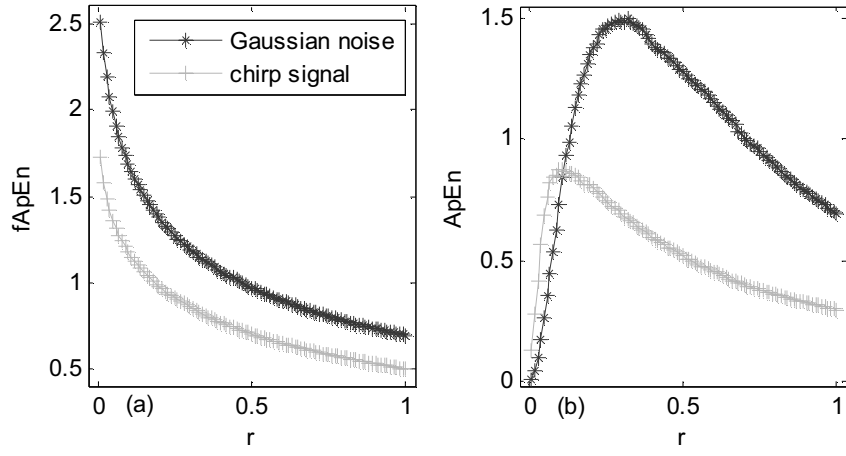


FIGURE 4.

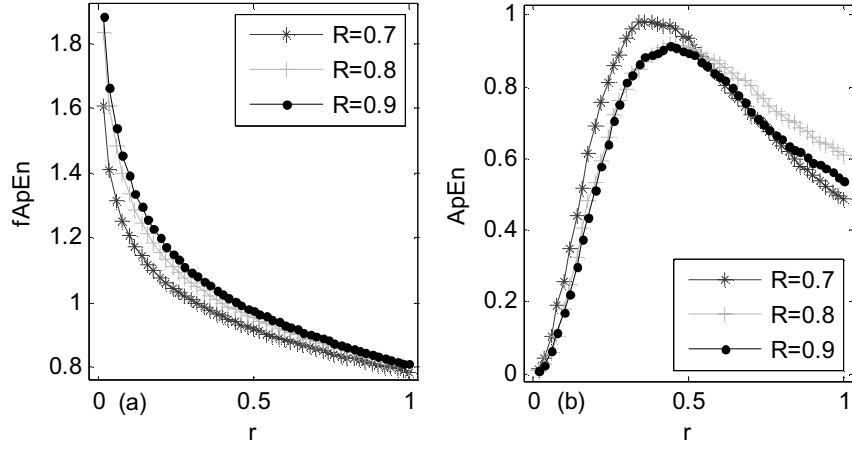


FIGURE 5.

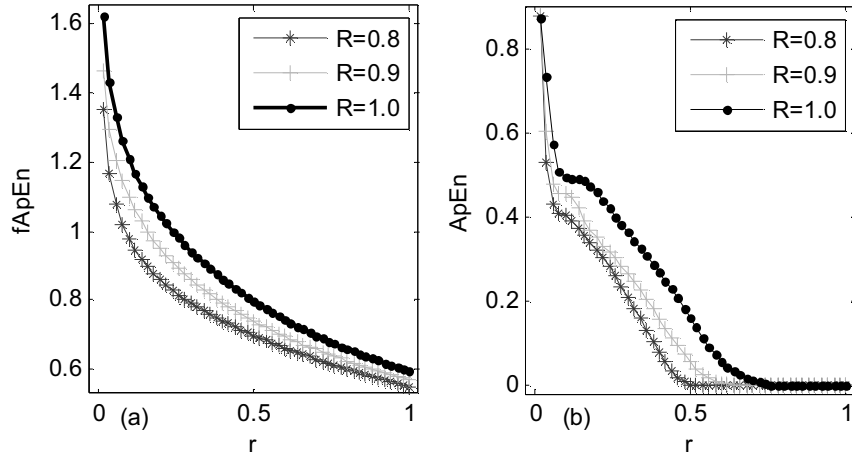


FIGURE 6.

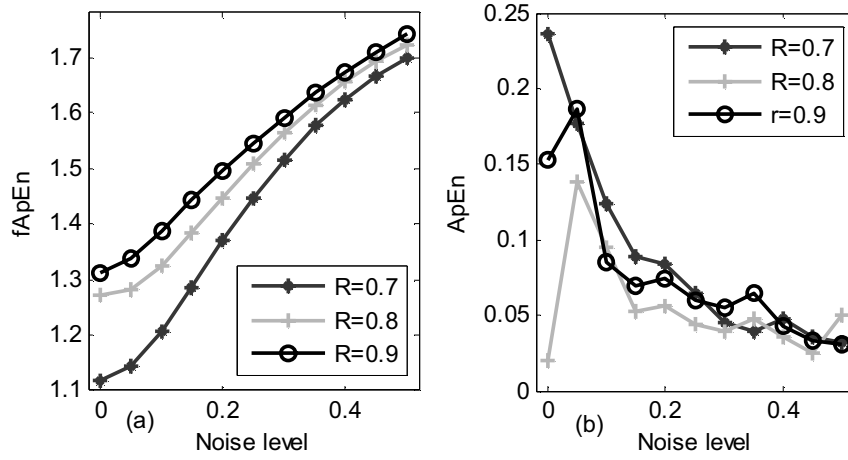


FIGURE 7.

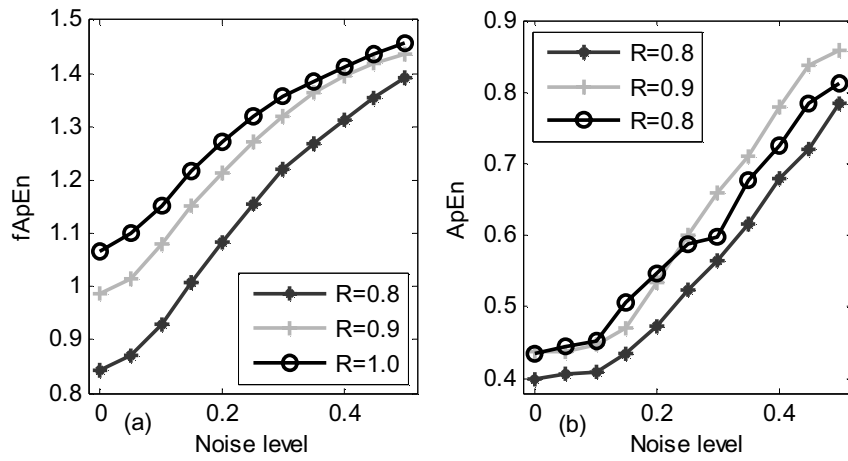


FIGURE 8.

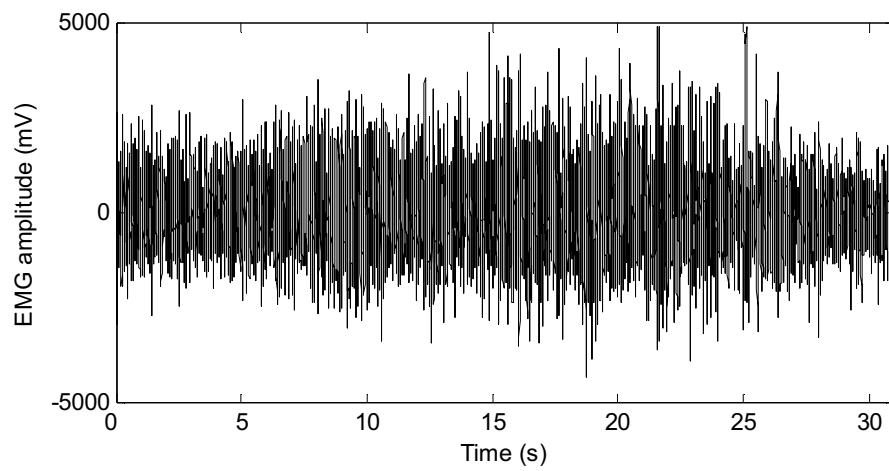


FIGURE 9.

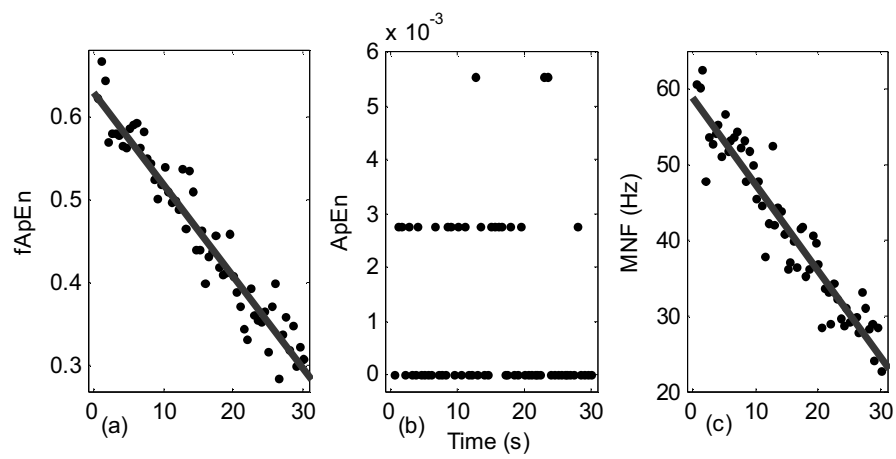


FIGURE 10.

1 Table caption

2 Table 1. The slope of the linear regression of $fApEn$ and MNF for each subject

3 TABLE 1. The slope of the linear regression lines of $fApEn$ and MNF for each subject

subject	$fApEn$	MNF
1	-0.0128	-0.0094
2	-0.0066	-0.0055
3	-0.0066	-0.0056
4	-0.0070	-0.0052
5	-0.0070	-0.0048
6	-0.0062	-0.0037
7	-0.0060	-0.0042
8	-0.0055	-0.0038
9	-0.0056	-0.0042
10	-0.0070	-0.0050
11	-0.0051	-0.0038
12	-0.0088	-0.0066
<i>Mean \pm std</i>	-0.0070 ± 0.0021	-0.0052 ± 0.0015

4
5